

**ORIGINAL  
RESEARCH**

A.M. Saindane  
M. Law  
Y. Ge  
G. Johnson  
J.S. Babb  
R.I. Grossman

# Correlation of Diffusion Tensor and Dynamic Perfusion MR Imaging Metrics in Normal-Appearing Corpus Callosum: Support for Primary Hypoperfusion in Multiple Sclerosis

**BACKGROUND AND PURPOSE:** Hypoperfusion of the normal-appearing white matter in multiple sclerosis (MS) may be related to ischemia or secondary to hypometabolism from wallerian degeneration (WD). This study evaluated whether correlating perfusion and diffusion tensor imaging (DTI) metrics in normal-appearing corpus callosum could provide support for an ischemic mechanism for hypoperfusion.

**MATERIALS AND METHODS:** Fourteen patients with relapsing-remitting MS (RRMS) and 17 control subjects underwent perfusion MR imaging and DTI. Absolute measures of cerebral blood volume (CBV), cerebral blood flow (CBF), and mean transit time (MTT) were calculated. Mean diffusivity (MD) and fractional anisotropy (FA) maps were computed from DTI data. After visual coregistration of perfusion and DTI images, regions of interest were placed in the genu, central body, and splenium of normal-appearing corpus callosum. Pearson product-moment correlation coefficients were calculated using mean DTI and perfusion measures in each region.

**RESULTS:** In the RRMS group, CBF and CBV were significantly correlated with MD in the splenium ( $r = 0.83$  and  $r = 0.63$ , respectively; both  $P < .001$ ) and in the central body ( $r = 0.86$  and  $r = 0.65$ , respectively; both  $P < .001$ ), but not in the genu ( $r = 0.23$  and  $0.25$ , respectively; both  $P$  is nonsignificant). No significant correlations were found between MTT and DTI measures or between FA and any perfusion measure in the RRMS group. No significant correlations between diffusion and perfusion metrics were found in control subjects.

**CONCLUSION:** In the normal-appearing corpus callosum of patients with RRMS, decreasing perfusion is correlated with decreasing MD. These findings are more consistent with what would be expected in primary ischemia than in secondary hypoperfusion from WD.

**M**ultiple sclerosis (MS) is a chronic inflammatory demyelinating disease of the central nervous system. Whereas MS has traditionally been characterized on conventional MR imaging by the presence of focal white matter lesions, it has become apparent that pathologic lesions are far from limited to these lesions. Histopathologic and biochemical studies have demonstrated that areas of grossly normal-appearing white matter (NAWM) distant from lesions can exhibit loss of myelin-specific proteins,<sup>1</sup> axonal damage and loss,<sup>2</sup> and perivascular infiltration by macrophages and T lymphocytes.<sup>3,4</sup> Advanced MR imaging techniques, such as proton MR spectroscopy<sup>5-7</sup> and magnetization transfer imaging,<sup>8-10</sup> have supported the concept of diffuse parenchymal abnormality in areas of NAWM on conventional MR imaging.

Using dynamic susceptibility contrast (DSC) enhanced perfusion MR imaging, it has been demonstrated that the NAWM of patients with MS exhibits significantly decreased perfusion compared with that of control subjects.<sup>11</sup> The underlying basis for this hypoperfusion is unknown, and may be related to ischemia from a primary vascular pathology, or secondary to decreased metabolic demand from processes such as wallerian degeneration (WD) of axons transected in distant lesions. This distinction has important implications for prog-

nosis and treatment, because ischemia may be an early and potentially reversible process, whereas hypometabolism secondary to axonal degeneration implies advanced disease and irreversibility.

Diffusion tensor imaging (DTI) is a technique that quantifies the amount of nonrandom water diffusion within tissues, providing information about processes such as ischemia and WD that can affect water diffusion as a result of microstructural damage. The diffusion tensor is calculated from images acquired with diffusion weighting gradients applied in at least 6 noncollinear directions and provides information on both the magnitude and directionality of water diffusion. Mean diffusivity (MD) calculated from the tensor provides a measure of average diffusion that is not influenced by patient positioning or fiber orientation. Higher values of MD indicate greater levels of diffusivity, indicating more space for diffusion to occur. The fractional anisotropy (FA) is a measure of the directionality of diffusion, and ranges from 0 to 1, with 0 reflecting completely isotropic diffusion, and 1 reflecting diffusion constrained to only 1 direction. Several studies have demonstrated altered tensor metrics in the setting of WD<sup>12-16</sup> and in the NAWM of patients with MS.<sup>17-21</sup>

Thus, the purpose of this study was to evaluate the relationship between perfusion and DTI changes in the normal-appearing corpus callosa of patients with relapsing-remitting MS (RRMS), with the hypothesis that correlations between perfusion and DTI measures would be more consistent with what would be expected in primary ischemia.

Received April 13, 2006; accepted after revision August 7.

From the Department of Radiology, New York University Medical Center, New York, NY.

Please address correspondence and reprints requests to: Meng Law, MD, Departments of Radiology and Neurosurgery, Mount Sinai Medical Center, One Gustave Levy Place, New York, NY 10029; e-mail: meng.law@gmail.com

## Materials and Methods

### Patients

Approval for this study was obtained from the Institutional Board of Research Associates, and informed consent was obtained from all patients. Fourteen patients with clinically definite RRMS<sup>22,23</sup> consecutively met inclusion criteria for this study. There were 6 male patients (median age, 43.6 years; range, 33.1–49.4 years) and 8 female patients (median age, 46.9 years; range, 36.7–60.0 years). Median age for all 14 patients was 45.7 (range, 33.1 to 60.0 years). All patients were receiving immunomodulating therapy with either interferon  $\alpha$ 1-a (Avonex; Biogen Ide, Cambridge, Mass) or Copolymer 1 (Copaxone; Teva, Petach Tikva, Israel). All patients were in a stable phase of disease, and no patients were receiving systemic corticosteroids during the study or in the 3 months preceding the study.

For comparison, 17 control patients were selected with no history of cerebrovascular disease, cardiovascular disease, evidence of small vessel ischemic disease, ischemic stroke, or substantial intracranial pathology on MR imaging. There were 6 male patients (median age, 49.5 years; range, 30.4–60.8 years) and 11 female patients (median age, 35.3 years; range, 23.0–65.7 years); the median age for all 17 control subjects was 39.0 (range, 23.0–65.7 years).

### MR Imaging

MR imaging was performed on a 1.5T Siemens clinical scanner. Patients with RRMS and control subjects each underwent conventional MR imaging, DTI, and DSC-MR imaging within the same imaging session. Localizing sagittal T1-weighted images of the brain were obtained, followed by contiguous 3-mm axial dual echo fast spin-echo proton attenuation and T2-weighted images (TR, 3400 ms; effective TE, 17,119 ms; NEX, 1), and contiguous 5-mm thick axial FLAIR images [TR, 9000; effective TE, 110 ms; TI, 2500 ms; matrix, 512  $\times$  256; FOV, 220  $\times$  220 mm]. DTI data were then obtained, followed by DSC-MR imaging and postcontrast axial (TR, 600 ms; TE, 14 ms; NEX, 1) T1-weighted images.

### DTI

Axial DTI data were acquired with a pulsed gradient, double spin-echo, echo-planar imaging method (TR, 4400 ms; TE, 100 ms; matrix, 200  $\times$  128; FOV, 220  $\times$  220 mm; 20 5-mm contiguous sections;  $b = 1000$  s/mm<sup>2</sup>). The pixel size for DTI is 1.72  $\times$  1.72 mm<sup>2</sup>. The double spin-echo technique is optimized to minimize eddy currents and geometric image distortion.<sup>24</sup> All axial imaging was acquired oriented parallel to the anterior commissure-posterior commissure plane. Diffusion weighting ( $b = 1000$  s/mm<sup>2</sup>) was applied along 6 noncollinear directions, ( $G_x, G_y, G_z$ ) = {(1,1,0), (1,0,1), (0,1,1), (1, -1, 0), (-1, 0, 1), (0,1, -1)}. For each of these 6 gradient directions, 4 acquisitions were averaged. One image without diffusion weighting ( $b = 0$ ) was acquired without averaging. This produced 7 images for each section.

### DSC-MR imaging

A series of 60 gradient-echo echo-planar images were acquired at 1-second intervals during the first pass of a standard dose (0.1 mmol/kg) bolus of gadopentetate dimeglumine (Magnevist; Berlex Laboratories, Wayne, NY). Seven 5-mm thick sections were acquired, positioned from the T2-weighted images to ensure coverage of a major vessel such as the anterior or middle cerebral arteries, as well as the corpus callosum. All patients had an 18- or 20-gauge intravenous catheter placed in the antecubital fossa for the purpose of contrast administration. The first 10 acquisitions were performed before con-

trast agent injection to establish a precontrast baseline. At the 10th acquisition, gadopentetate dimeglumine (0.1 mmol/kg) was injected with a power injector (Medrad, Indianola, Pa) at a rate of 5 mL/s, immediately followed by a bolus injection of saline (total of 20 mL at 5 mL/s). The specific imaging parameters are: TR, 1000 ms; TE, 54 ms; FOV, 230  $\times$  230 mm; section thickness, 5 mm; matrix, 128  $\times$  128; in-plane voxel size, 1.8  $\times$  1.8 mm; intersection gap, 0%–30%; flip angle, 30°; signal intensity bandwidth, 1470 Hz/pixel. The methods for acquiring perfusion data from a set of DSC enhanced echo-planar images have been described previously.<sup>25–28</sup>

### Image Processing and Evaluation

Data processing was performed off-line using a Sun Ultra 10 workstation with programs developed in-house using the C and IDL (RSI, Boulder, Colo) programming languages. Six maps of the apparent diffusion coefficient were computed, from which the diffusion tensor was calculated. From this tensor, eigenvalues and eigenvectors were derived. The FA and the MD trace were computed from these measures for each voxel by standard algorithms.<sup>29</sup> MD and FA values were calculated on a pixel-by-pixel basis to form maps for each section.

Absolute cerebral blood volume (CBV), cerebral blood flow (CBF), and mean transit time (MTT) were calculated using the method of Rempp et al.<sup>26,27</sup> In brief, tissue concentration is found from the change in relaxation rate that occurs during bolus passage. The tissue concentration that results from an idealized, instantaneous bolus is then found by deconvolving the actual tissue concentration with the arterial input function (AIF). Deconvolution was carried out by singular value decomposition.<sup>27,28</sup> The AIF was found using an automated method similar to that described by Rempp et al.<sup>26,30</sup> The minimum signal intensity, corresponding to the bolus peak, is found in each pixel within the head. The average signal intensity drop and average bolus arrival time are then calculated for all pixels. Pixels where the bolus arrives early and where the signal intensity drop is larger than average are assumed to be within arteries. The AIF is found by averaging the signals from all such pixels.

After visual coregistration of the FA map, MD map, and perfusion MR images, 2 regions of interest (ROIs) were placed in the central body and in bilateral areas of genu and splenium of the corpus callosum, as shown in Fig 1. ROIs were fixed in size (radius = 1 image pixel, 1.8 mm) and placed so as to avoid arterial or venous structures on the perfusion images. Furthermore, the ROIs were placed after visual coregistration with the axial T2-weighted and FLAIR images to ensure lesions were not included in the ROI. This generated measures of FA, MD, CBV, CBF, and MTT for each of the ROIs.

### Statistical Analysis

The strength of the association between DTI and perfusion measures within each area of the corpus callosum was estimated for both the RRMS group and control group using Pearson product-moment correlation coefficients. Because each subject provided multiple assessments of each metric within each area (each measure was assessed at multiple locations within each area), there were statistical dependencies (within-subject correlations) among observations that had to be accounted for in the statistical analysis. Consequently, mixed-model least-squares regression was used to assess the statistical significance of the associations between DTI and perfusion measures and to test whether the correlation between a given pair of metrics (eg, CBV with FA) in a given area was different for patients than it is for controls, while adjusting for the correlation among observations provided by the same subject and the potential confounding effects of age and sex.

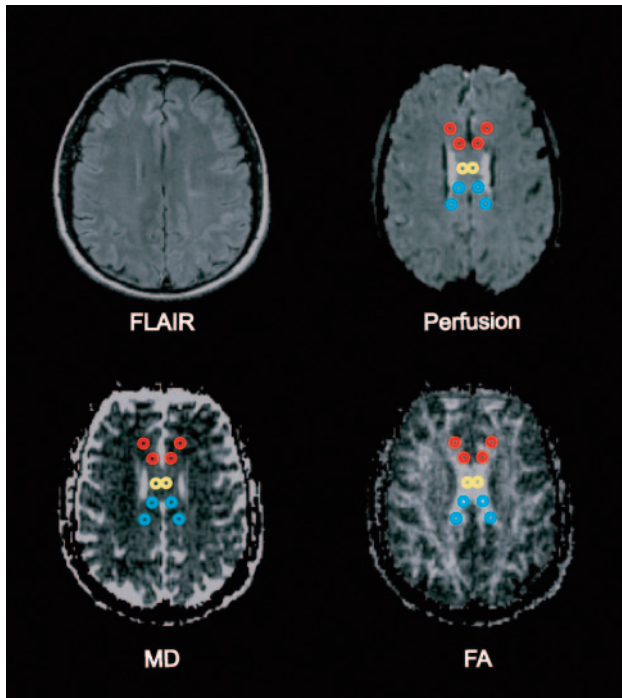


**Fig 1.** Fluid-attenuated inversion recovery image, perfusion image, MD map, and FA map showing placement of ROIs within the genu (red), central body (yellow), and splenium (blue) of the corpus callosum.

The mixed model included subject age and sex as fixed numeric and classification factors, respectively, assumed that the observations derived for a given metric were correlated or independent when derived for the same subject or different subjects, respectively, and allowed the variance of the metric to differ across both subject groups and areas of the corpus callosum.

## Results

The results for correlations between MD and perfusion measures are shown in Table 1. In RRMS patients, CBF was significantly correlated with MD in the central body ( $r = 0.86$ ;  $P < .0001$ ) and splenium ( $r = 0.83$ ;  $P < .0001$ ) of the corpus callosum. CBV was also significantly correlated with MD in the central body ( $r = 0.63$ ;  $P = .0046$ ) and splenium ( $r = 0.65$ ;  $P < .0001$ ) of the corpus callosum. In the genu of the corpus callosum, no significant correlations were found between MD and either CBF or CBV, and no significant correlations were present between MD and MTT in any of the areas of corpus callosum of patients with RRMS. The control group did not demonstrate significant correlations between MD and any perfusion measures in any of the areas of corpus callosum examined. The results for correlations between FA and perfusion measures are shown in Table 2. No significant correlations were present between FA and any of the perfusion metrics in any of the areas of corpus callosum of both patients with RRMS and control subjects.

The  $P$  values listed in Tables 1 and 2 were determined from the mixed-model analysis to account for within-subject correlations. These  $P$  values were used to test whether the correlation between a given pair of measures is different for patients with RRMS than it is for control subjects. Indicating that the significant correlations found in Table 1 were different between the RRMS group and the control group, significant inter-

actions were found between MD and CBV in the central body ( $P = .037$ ) and splenium ( $P = .018$ ), and between MD and CBF in the central body ( $P = .045$ ) and splenium ( $P = .017$ ). A significant interaction was also found between FA and CBF within the central body of the corpus callosum ( $P = .047$ ). This significant interaction occurred because the correlation was positive among patients with RRMS, negative among control subjects, and moderate in magnitude within both groups (ie, although neither correlation was significant individually, the difference between them was large). No other significant interactions were found between the RRMS and control groups with respect to correlations between perfusion and DTI metrics.

## Discussion

Numerous histopathologic and biochemical studies have demonstrated that in addition to the characteristic discrete white matter lesions found in patients with MS, there is diffuse abnormality involving grossly NAWM. Findings in the NAWM include decreased myelin-specific protein,<sup>1</sup> diffuse astrogliosis,<sup>31</sup> and infiltration by macrophages and T lymphocytes.<sup>3,4</sup> Although MS has prototypically been characterized as a demyelinating disease, axonal damage, including axonal transection and decreased fiber attenuation, has been demonstrated in both lesions as well as within the NAWM.<sup>2,32</sup>

Advanced MR imaging studies have demonstrated abnormalities in areas of white matter that are not visualized on conventional MR imaging. MR spectroscopy studies have found metabolic alterations within the NAWM. *N*-acetylaspartate is a neuronal marker that is commonly decreased within MS lesions and has also been found to be decreased in regions of NAWM,<sup>5-7</sup> signifying diffuse axonal loss or dysfunction. Loss of macromolecular organization, such as when myelin is fragmented or destroyed, influences the transfer of magnetization from macromolecules to free water, and this magnetization can be measured using MR as the magnetization transfer ratio (MTr). In patients with MS, the MTr is significantly reduced in areas of NAWM,<sup>8-10</sup> supporting the concept of diffuse parenchymal macrostructural abnormality.

Using DSC enhanced perfusion MR imaging, Law et al<sup>11</sup> demonstrated significant hypoperfusion in the NAWM of RRMS patients compared with control subjects; however, a specific mechanism for the hypoperfusion could not be suggested on the basis of that study. Fundamentally, there are 2 possible causes for NAWM hypoperfusion, which can be categorized as primary or secondary. In the first scenario, a primary vascular pathologic lesion results in decreased perfusion in the NAWM with consequent ischemic parenchymal injury. In the second scenario, axonal damage in MS lesions leads to WD of axons traversing distant areas of white matter, resulting in decreased axonal attenuation, regional hypometabolism, and secondary hypoperfusion of the NAWM. The distinction between these mechanisms has potentially important implications, because ischemia may be an early and potentially reversible finding, whereas hypometabolism from axonal degeneration would represent advanced and irreversible disease.

DTI has proved to be a valuable tool for investigating the integrity of white matter microstructure that cannot be assessed by conventional MR imaging and has been used to study both ischemia and WD. Parameters such as the MD

**Table 1: Pearson correlation coefficients for the association of MD with perfusion measures within each area of the corpus callosum of patients with RRMS and control subjects**

Location	CBV		CBF		MTT	
	<i>r</i>	<i>P</i>	<i>r</i>	<i>P</i>	<i>r</i>	<i>P</i>
RRMS ( <i>n</i> = 14)						
Genu	0.25	.87	0.23	.89	0.08	.73
Body	0.63	.046	0.86	<.0001	-0.39	.08
Splenium	0.65	<.0001	0.83	<.0001	-0.33	.08
Control ( <i>n</i> = 17)						
Genu	-0.09	.74	0.04	.64	-0.15	.33
Body	-0.01	.72	0.17	.81	-0.21	.61
Splenium	-0.03	.54	-0.004	.82	-0.11	.73

**Note:**—MD, mean diffusivity; RRMS, relapsing-remitting multiple sclerosis; CBF, cerebral blood flow; CBV, cerebral blood volume; MTT, mean transit time. Statistical significance accepted at *P* < .05.

**Table 2: Pearson correlation coefficients for the association of FA with perfusion measures within each area of the corpus callosum of patients with RRMS and control subjects**

Location	CBV		CBF		MTT	
	<i>r</i>	<i>P</i>	<i>r</i>	<i>P</i>	<i>r</i>	<i>P</i>
RRMS ( <i>n</i> = 14)						
Genu	-0.38	.07	-0.24	.45	-0.02	.99
Body	0.44	.08	0.28	.09	-0.31	.18
Splenium	-0.04	.74	-0.11	.90	-0.01	.99
Control ( <i>n</i> = 17)						
Genu	-0.02	.77	-0.05	.80	-0.01	.87
Body	-0.06	.67	-0.17	.26	0.08	.59
Splenium	-0.01	.73	-0.05	.82	0.12	.56

**Note:**—FA, fractional anisotropy; RRMS, relapsing remitting multiple sclerosis; CBF, cerebral blood flow; CBV, cerebral blood volume; MTT, mean transit time. Statistical significance accepted at *P* < .05.

averaged over 3 orthogonal directions measure the magnitude of diffusion of water molecules, whereas diffusion anisotropy indices, such as FA, indicate the degree of deviation from isotropic diffusion of water molecules. In studies of acute ischemic stroke, MD has been found to be decreased in the immediate setting,<sup>33,34</sup> related to acute cellular swelling. The MD later increases toward normal values and finally becomes elevated in the chronic phase, thought to represent destruction of membrane integrity and progression toward tissue necrosis.<sup>35</sup> Fractional anisotropy progressively decreases in the white matter in the setting of ischemia,<sup>33,36</sup> again attributed to ongoing tissue destruction.

Studies have demonstrated DTI changes related to WD in the setting of ischemic stroke.<sup>12,13</sup> Thomalla et al<sup>14</sup> found decreases in FA reflecting early WD in the cerebral peduncle of the affected side as early as 2–16 days after ischemic stroke, whereas maps of the orientationally averaged diffusivity did not reveal obvious changes. Months to years after ischemic stroke, FA becomes chronically decreased, and MD increases slightly along the pyramidal tract on the affected side below the primary lesion.<sup>12,15,16</sup> This is thought to be related to fibrosis and atrophy of affected connected fiber tracts.<sup>37</sup>

In this study, we correlated DTI and perfusion MR metrics in the normal-appearing corpus callosa of patients with MS and control subjects to further elucidate the basis for hypoperfusion in MS. We chose the corpus callosum as the focus for evaluation because it is the most highly organized interhemispheric structure in the brain,<sup>38</sup> providing a sensitive area for evaluation of subtle changes in DTI measures. In the MS group, we found highly significant large-magnitude correlations between perfusion measures and MD, specifically that

decreasing CBF was associated with decreasing MD (increased diffusion restriction) and not significantly correlated with FA. We interpret these findings as support for primary hypoperfusion (ischemia) in MS. In the setting of primary ischemia, areas with the lowest perfusion would be expected to have the most restricted diffusion (the most decreased mean diffusivity), with possibly only slight decreases in FA, consistent with the findings of this study. In secondary hypoperfusion related to WD, the most hypometabolic/hypoperfused areas should in theory have the lowest axonal fiber attenuation and would thus be expected to have the most increased MD and most decreased FA. The mixed model analysis demonstrated that the significant correlations between DTI and perfusion measures are not present in control subjects, suggesting that they are related to the disease process.

This study does not refute the presence or importance of WD in MS; however, it suggests that hypoperfusion is due to alternative (primary vascular) pathologic conditions. Indeed, considerable evidence supports the idea that WD does occur in MS and specifically within the corpus callosum. Recent evidence from a quantitative postmortem study of patients with MS demonstrated a significant reduction of axonal attenuation and volume in areas of corpus callosum that appeared grossly normal.<sup>32</sup> Several studies of diffusion properties of the NAWM in MS have demonstrated findings of increased MD and decreased FA,<sup>17-20</sup> as is seen in WD from ischemic stroke. However, it is important to consider that the end point of tissue destruction of disparate pathologic conditions could lead to a similar pattern of DTI findings. Although studies have shown that DTI abnormalities in the NAWM correlate with DTI abnormalities within lesions,<sup>21,39</sup> this may simply

reflect an underlying primary pathologic condition responsible for both lesions and NAWM damage and does not necessarily indicate that WD is primarily from lesions. In theory, diffuse ischemic injury in MS could also lead to WD of axons in the NAWM. In fact, microscopic ischemic injury in the corpus callosum, given its central location and high axonal fiber attenuation, could lead to extensive bihemispheric WD.

Further arguing against WD from lesions as the basis for NAWM hypoperfusion is that abnormalities in the NAWM have been described early in the course of disease in patients with MS without substantial lesion loads. De Stefano et al<sup>40</sup> showed that cerebral *N*-acetylaspartate/creatinine and MTr values are diffusely decreased in patients with MS with early disease, no significant disability, and low demyelinating lesion load, suggesting that axonal injury begins very early in the course of MS. Metabolic abnormalities have been detected in the corpus callosum using MR spectroscopy at the earliest stage of clinically isolated syndrome suggestive of MS, before atrophy and lesions are detected.<sup>41</sup>

It could be argued that rather than WD from distant lesions, decreased perfusion in NAWM could be related to widespread parenchymal damage below the resolution of conventional MR imaging from a nonischemic etiology. While diffuse nonischemic parenchymal injury could lead to hypoperfusion secondary to hypometabolism and similar findings of increased MD and decreased FA within the NAWM, the expected correlations between perfusion and DTI measures would be similar to that found in WD, with the most hypometabolic/hypoperfused areas containing the most parenchymal damage demonstrating highest MD and lowest FA.

Considerable histopathologic evidence supports a primary vascular pathologic lesion in MS. Studies have described perivascular inflammatory changes such as lymphocytic infiltration and edematous onion-skin changes of vein walls in NAWM lacking adjacent parenchymal inflammation, suggesting that MS could represent a form of subacute or chronic vasculitis.<sup>31,42</sup> Vascular occlusion in MS was described on histopathologic examination by Putnam<sup>43,44</sup> in the 1930s and later by Wakefield et al,<sup>45</sup> who demonstrated fibrin deposition and thrombosis of vessels in the absence of cellular infiltration, suggesting that thrombosis of small veins and capillaries could represent an ischemic basis for disease. More recent studies have demonstrated the presence of extensive oligodendrocyte apoptosis<sup>46</sup> and preferential loss of myelin-associated glycoprotein,<sup>47</sup> which is suggestive of hypoxic-ischemic-type tissue injury.

It is not clear why correlations between perfusion and DTI metrics were found in the body and splenium of the corpus callosum, but not in the genu; however, this could be related to differences in fiber composition of the corpus callosum. Thin fibers seem to be most susceptible to injury in MS,<sup>48</sup> and there is a higher attenuation of thin fibers in the splenium than in the genu.<sup>49</sup> Although vascular changes in MS would be expected to diffusely affect the corpus callosum, it is possible that larger fibers in the genu would be more resistant to ischemic injury.

Although we interpret our findings of significant correlations between DTI and perfusion measures as significant, there are limitations to this study. Visual coregistration of the perfusion images and DTI maps can lead to errors from mis-

registration. Although changes in MD would not be as subject to variability over small distances, FA is highly dependent on the area of corpus callosum sampled, and slight differences in ROI placement could partly explain a lack of correlation between perfusion measures and FA in both MS and control groups. Another limitation of the study related to visual coregistration is the inability to measure DTI and perfusion parameters in a blinded fashion, because simultaneous placement of corresponding ROIs was required. However, measurements from the perfusion analysis were not visible when placing ROIs on the DTI images and were obtained simultaneously for all ROIs so as to limit bias from manipulation of ROI placement.

The perfusion algorithm used has inherent limitations and is accurate only if there is negligible delay and dispersion in the bolus between the arteries where the AIF is measured and the tissue of interest. Delays and dispersion introduce errors into the calculation of perfusion parameters<sup>50,51</sup>; however, these errors should be minimal, because the AIF is estimated close to the site of the perfusion measurements. The effect of the disease process itself on the AIF is also not known, though at this time it seems that there is relative sparing of the major arteries in the vasculitic process and hence the AIF may not be greatly affected in MS. Finally, all patients in the MS group were undergoing chronic immunomodulating therapy, possibly decreasing the inflammatory component of the disease process within the NAWM and affecting both DTI and perfusion measures.

The results of this study correlating DTI and perfusion changes are more consistent with what would be expected in primary ischemia than in secondary hypoperfusion from WD. Further investigation, including larger and longitudinal studies are warranted to additionally support the concept of ischemic injury in MS. A better understanding of the role of ischemia could aid in predicting clinical course, monitoring response to therapy, and designing novel targets for therapeutic intervention for MS.

## Conclusions

In areas of normal-appearing corpus callosum of patients with RRMS, decreasing perfusion is correlated with decreasing MD and is not significantly correlated with FA. These findings support the concept of primary ischemia in MS rather than secondary hypoperfusion as a result of WD.

## References

1. Trotter JL, Wegescheide CL, Garvey WF, et al. **Studies of myelin proteins in multiple sclerosis brain tissue.** *Neurochem Res* 1984;9:147–52
2. Trapp BD, Peterson J, Ransohoff RM, et al. **Axonal transection in the lesions of multiple sclerosis.** *N Engl J Med* 1998;338:278–85
3. Traugott U, Reinherz EL, Raine CS. **Multiple sclerosis. Distribution of T cells, T cell subsets and Ia-positive macrophages in lesions of different ages.** *J Neuroimmunol* 1983;4:201–21
4. Adams CW. **Pathology of multiple sclerosis: progression of the lesion.** *Br Med Bull* 1977;33:15–20
5. Narayanan S, Fu L, Pioro E, et al. **Imaging of axonal damage in multiple sclerosis: spatial distribution of magnetic resonance imaging lesions.** *Ann Neurol* 1997;41:385–91
6. Husted CA, Goodin DS, Hugg JW, et al. **Biochemical alterations in multiple sclerosis lesions and normal-appearing white matter detected by in vivo 31P and 1H spectroscopic imaging.** *Ann Neurol* 1994;36:157–65
7. Davie CA, Barker GJ, Thompson AJ, et al. **1H magnetic resonance spectroscopy of chronic cerebral white matter lesions and normal appearing white matter in multiple sclerosis.** *J Neurol Neurosurg Psychiatry* 1997;63:736–42

8. Filippi M, Campi A, Dousset V, et al. A magnetization transfer imaging study of normal-appearing white matter in multiple sclerosis. *Neurology* 1995;45:478–82
9. Loevner LA, Grossman RI, Cohen JA, et al. Microscopic disease in normal-appearing white matter on conventional MR images in patients with multiple sclerosis: assessment with magnetization-transfer measurements. *Radiology* 1995;196:511–15
10. Ge Y, Grossman RI, Udupa JK, et al. Magnetization transfer ratio histogram analysis of normal-appearing gray matter and normal-appearing white matter in multiple sclerosis. *J Comput Assist Tomogr* 2002;26:62–68
11. Law M, Saindane AM, Ge Y, et al. Microvascular abnormality in relapsing-remitting multiple sclerosis: perfusion MR imaging findings in normal-appearing white matter. *Radiology* 2004;231:645–52
12. Thomalla G, Glauche V, Weiller C, et al. Time course of wallerian degeneration after ischaemic stroke revealed by diffusion tensor imaging. *J Neurol Neurosurg Psychiatry* 2005;76:266–68
13. Khong PL, Zhou LJ, Ooi GC, et al. The evaluation of Wallerian degeneration in chronic paediatric middle cerebral artery infarction using diffusion tensor MR imaging. *Cerebrovasc Dis* 2004;18:240–47
14. Thomalla G, Glauche V, Koch MA, et al. Diffusion tensor imaging detects early wallerian degeneration of the pyramidal tract after ischemic stroke. *NeuroImage* 2004;22:1767–74
15. Werring DJ, Toosy AT, Clark CA, et al. Diffusion tensor imaging can detect and quantify corticospinal tract degeneration after stroke. *J Neurol Neurosurg Psychiatry* 2000;69:269–72
16. Pierpaoli C, Barnett A, Pajevic S, et al. Water diffusion changes in wallerian degeneration and their dependence on white matter architecture. *Neuroimage* 2001;13:1174–85
17. Werring DJ, Clark CA, Barker GJ, et al. Diffusion tensor imaging of lesions and normal-appearing white matter in multiple sclerosis. *Neurology* 1999;52:1626–32
18. Filippi M. Linking structural, metabolic and functional changes in multiple sclerosis. *Eur J Neurol* 2001;8:291–97
19. Bammer R, Keeling SL, Augustin M, et al. Improved diffusion-weighted single-shot echo-planar imaging (EPI) in stroke using sensitivity encoding (SENSE). *Magn Reson Med* 2001;46:548–54
20. Guo AC, MacFall JR, Provenzale JM. Multiple sclerosis: diffusion tensor MR imaging for evaluation of normal-appearing white matter. *Radiology* 2002;222:729–36
21. Werring DJ, Clark CA, Droogan AG, et al. Water diffusion is elevated in widespread regions of normal-appearing white matter in multiple sclerosis and correlates with diffusion in focal lesions. *Mult Scler* 2001;7:83–89
22. Poser CM, Paty DW, Scheinberg L, et al. New diagnostic criteria for multiple sclerosis: guidelines for research protocols. *Ann Neurol* 1983;13:227–31
23. Lublin FD, Reingold SC. Defining the clinical course of multiple sclerosis: results of an international survey. National Multiple Sclerosis Society (USA) Advisory Committee on Clinical Trials of New Agents in Multiple Sclerosis. *Neurology* 1996;46:907–11
24. Reese TG, Heid O, Weisskoff RM, et al. Reduction of eddy-current-induced distortion in diffusion MRI using a twice-refocused spin echo. *Magn Reson Med* 2003;49:177–82
25. Knopp EA, Cha S, Johnson G, et al. Glial neoplasms: dynamic contrast-enhanced T2\*-weighted MR imaging. *Radiology* 1999;211:791–98
26. Rempp KA, Brix G, Wenz F, et al. Quantification of regional cerebral blood flow and volume with dynamic susceptibility contrast-enhanced MR imaging. *Radiology* 1994;193:637–41
27. Ostergaard L, Weisskoff RM, Chesler DA, et al. High resolution measurement of cerebral blood flow using intravascular tracer bolus passages. Part I: mathematical approach and statistical analysis. *Magn Reson Med* 1996;36:715–25
28. Ostergaard L, Sorensen AG, Kwong KK, et al. High resolution measurement of cerebral blood flow using intravascular tracer bolus passages. Part II: experimental comparison and preliminary results. *Magn Reson Med* 1996;36:726–36
29. Basser PJ. Inferring microstructural features and the physiological state of tissues from diffusion-weighted images. *NMR Biomed* 1995;8:333–44
30. Carroll TJ, Rowley HA, Houghton VM. Automatic calculation of the arterial input function for cerebral perfusion imaging with MR imaging. *Radiology* 2003;227:593–600
31. Allen IV, McKeown SR. A histological, histochemical and biochemical study of the macroscopically normal white matter in multiple sclerosis. *J Neurol Sci* 1979;41:81–91
32. Evangelou N, Esiri MM, Smith S, et al. Quantitative pathological evidence for axonal loss in normal appearing white matter in multiple sclerosis. *Ann Neurol* 2000;47:391–95
33. Munoz Maniega SM, Bastin ME, Armitage PA, et al. Temporal evolution of water diffusion parameters is different in grey and white matter in human ischaemic stroke. *J Neurol Neurosurg Psychiatry* 2004;75:1714–18
34. Buffon F, Molko N, Herve D, et al. Longitudinal diffusion changes in cerebral hemispheres after MCA infarcts. *J Cereb Blood Flow Metab* 2005;25:641–50
35. Pierpaoli C, Righini A, Linfante I, et al. Histopathologic correlates of abnormal water diffusion in cerebral ischemia: diffusion-weighted MR imaging and light and electron microscopic study. *Radiology* 1993;189:439–48
36. Sorensen AG, Wu O, Copen WA, et al. Human acute cerebral ischemia: detection of changes in water diffusion anisotropy by using MR imaging. *Radiology* 1999;212:785–92
37. Johnson AC, McNabb, Rossiter RJ. Chemistry of wallerian degeneration; a review of recent studies. *Arch Neurol Psychiatry* 1950;64:105–21
38. Tomasch J. Size, distribution, and number of fibres in the human corpus callosum. *Anat Rec* 1954;119:119–35
39. Ciccarelli O, Werring DJ, Barker GJ, et al. A study of the mechanisms of normal-appearing white matter damage in multiple sclerosis using diffusion tensor imaging—evidence of Wallerian degeneration. *J Neurol* 2003;250:287–92
40. De Stefano N, Narayanan S, Francis SJ, et al. Diffuse axonal and tissue injury in patients with multiple sclerosis with low cerebral lesion load and no disability. *Arch Neurol* 2002;59:1565–71
41. Ranjeva JP, Pelletier J, Confort-Gouny S, et al. MRI/MRS of corpus callosum in patients with clinically isolated syndrome suggestive of multiple sclerosis. *Mult Scler* 2003;9:554–65
42. Adams CW, Poston RN, Buk SJ, et al. Inflammatory vasculitis in multiple sclerosis. *J Neurol Sci* 1985;69:269–83
43. Putnam TJ. Evidences of vascular occlusion in multiple sclerosis and encephalomyelitis. *Arch Neurol Neuropsychol* 1935;32:1298–321
44. Putnam TJ. The pathogenesis of multiple sclerosis: a possible vascular factor. *N Engl J Med* 1933;209:786–90
45. Wakefield AJ, More LJ, Difford J, et al. Immunohistochemical study of vascular injury in acute multiple sclerosis. *J Clin Pathol* 1994;47:129–33
46. Barnett MH, Prineas JW. Relapsing and remitting multiple sclerosis: pathology of the newly forming lesion. *Ann Neurol* 2004;55:458–68
47. Aboul-Enein F, Rauschka H, Kornek B, et al. Preferential loss of myelin-associated glycoprotein reflects hypoxia-like white matter damage in stroke and inflammatory brain diseases. *J Neuropathol Exp Neurol* 2003;62:25–33
48. Evangelou N, Konz D, Esiri MM, et al. Size-selective neuronal changes in the anterior optic pathways suggest a differential susceptibility to injury in multiple sclerosis. *Brain* 2001;124:1813–20
49. Aboitiz F, Scheibel AB, Fisher RS, et al. Fiber composition of the human corpus callosum. *Brain Res* 1992;598:143–53
50. Calamante F, Gadian DG, Connelly A. Delay and dispersion effects in dynamic susceptibility contrast MRI: simulations using singular value decomposition. *Magn Reson Med* 2000;44:466–73
51. Calamante F, Gadian DG, Connelly A. Quantification of perfusion using bolus tracking magnetic resonance imaging in stroke: assumptions, limitations, and potential implications for clinical use. *Stroke* 2002;33:1146–51